Title:

A combined kinematic and kinetic analysis at the residuum/socket interface of a knee-disarticulation amputee

Authors:

Jinghua Tang[1], Michael McGrath[1], Nick Hale[1], Liudi Jiang[1], Dan Bader[2], Piotr Laszczak[1], David Moser[3], Saeed Zahedi[3]

[1]Faculty of Engineering and the Environment, University of Southampton, So17 1BJ, UK

[2]Faculty of Health Sciences, University of Southampton, SO17 1BJ, UK

[3]Chas A Blatchford & Sons Ltd., Endolite Technology Centre, Kingsland Business Park, Basingstoke, RG24 8PZ, UK

Corresponding Author

Professor Liudi Jiang

Email: L. Jiang@soton.ac.uk

Address: Faculty of Engineering and the Environment, University of Southampton, SO17 1BJ, UK

Abstract

Background

The bespoke interface between a lower limb residuum and a prosthetic socket is critical for an amputee's comfort and overall rehabilitation outcomes. Analysis of interface kinematics and kinetics is important to gain full understanding of the interface biomechanics, which could aid clinical socket fit, rehabilitation and amputee care. This pilot study aims to investigate the dynamic correlation between kinematic movement and kinetic stresses at the interface during walking tests on different terrains.

Methods

One male, knee disarticulation amputee participated in the study. He was asked to walk on both a level surface and a 5° ramped surface. The movement between the residuum and the socket was evaluated by the angular and axial couplings, based on the outputs from a 3D motion capture system. The corresponding kinetic stresses at anterior-proximal (AP), posterior-proximal (PP) and anterior-distal (AD) locations of the residuum were measured, using individual stress sensors.

Findings

Approximately 8° of angular coupling and up to 32mm of axial coupling were measured when walking on different terrains. The direction of the angular coupling shows strong correlation with the pressure difference between the PP and AP sensors. Higher pressure was obtained at the PP location than the AP location during stance phase, associated with the direction of the angular coupling. A strong correlation between axial coupling length, L, and longitudinal shear was also evident at the PP and AD locations i.e. the shortening of L corresponds to the increase of shear in the proximal direction. Although different terrains did not affect these correlations in principle, interface kinematic and kinetic values suggested that gait changes can induce modifications to the interface biomechanics.

Clinical relevance

It is envisaged that the reported techniques could be potentially used to provide combined kinematics and kinetics for the understanding of biomechanics at the residuum/socket interface, which may play an important role in the clinical assessment of prosthetic component settings, including socket fit quality.

1 Introduction

A prosthetic socket is an essential part of any lower limb prosthesis, which is custom-made and provides attachment between the rest of the prosthesis and the residuum of a lower limb amputee. The critical interface, formed by the residuum and the socket, is well recognised to play an important role in amputee comfort, residuum tissue health and overall rehabilitation outcomes [1, 2]. Consequently, the biomechanical understanding of this interface has attracted significant interest [3]. In the past 60 years, a number of studies have sought to assess the kinematics and kinetics at this interface. For example, in order to evaluate the real-time interface kinematics, various imaging techniques involving X-ray [4-6], Dynamic Roentgen Stereogrammetric Analysis (DRSA) [7], ultrasound technology [8] and non-contact sensors [9], have been exploited and these have reported up to 57mm of axial coupling [10] and 10° of angular coupling [8] in a gait cycle (GC). Equally, in order to evaluate the real-time interface kinetics, interface stress sensors such as strain gauge-based sensors [11-13] and magneto-resistive sensors [14], have been inserted at the residuum/socket interface and up to 350kPa pressure (i.e. stress acting normal to skin) and 80kPa shear (i.e. stress acting parallel to the skin) have been reported during amputee walking tests [14, 15].

Despite all these studies, imaging-based technologies for kinematic evaluation are either not widely available, expensive or can expose the patients to radiation. This limits their accessibility in a prosthetic clinical setting. To address this challenge, we have recently developed a new and clinically accessible method to characterise the 3D dynamic kinematic coupling at the residuum/socket interface using a 3D motion capture dataset [16]. Preliminary results obtained from walking tests of a trans-femoral amputee suggested up to 11° of angular coupling in the sagittal plane and 35mm of axial coupling, aligning well with the findings of other studies [8, 17]. For the interface kinetic studies reported to date, most stress sensors reported were only able to measure pressure, including a few commercial systems e.g. Tekscan™ F-Socket system and Novel™. The few reported combined pressure and shear sensors were either too bulky, required socket modifications to insert at the interface [14], or were built on rigid substrates [18, 19], all of which precluded their use at the interface of a tight fitting socket. We have recently developed a unique thin and flexible sensor, which can be directly applied at residuum/socket interface to provide combined pressure and shear measurement during ambulation [20, 21].

It is well known in the field of lower limb biomechanics that, in the case of trans-femoral amputees, the relative kinematic movement between the femur and the socket determines the forces or stress profiles that the socket exerts on the residuum, as a function of GC [3, 22]. For example, it has been suggested [3, 22] that the distal femur moves posteriorly for knee stabilisation and results in higher pressures in the posterior-

distal region of the residuum in early stance phase. In late stance phase, in order to initiate knee flexion, the distal femur presses anteriorly causing higher pressure at the anterior-distal location. Sanders, et al. [9] also highlighted the importance of correlating the dynamic residuum axial displacement in the socket with the corresponding interface pressure and shear stresses in order to provide a combined assessment, which is critical for clinical outcome measures.

Despite the essential association between the kinematic and kinetic information for the evaluation of interface biomechanics, there is a paucity of studies combining assessments of residuum/socket interface biomechanics. This is largely due to the lack of effective and clinically applicable means for these assessments.

In the present study, we report kinematic and kinetic biomechanical results at the residuum/socket interface based on pilot studies, involving a knee-disarticulation amputee. Various tests were conducted, including walking on level surfaces and ascending and descending ramped surfaces, while 3D motion capture data and interface stress sensors output were collected simultaneously and subsequently analysed. The aim of this pilot study was to demonstrate a new method, which is the first of its kind, for capturing the combined kinematics and kinetics of the residuum/socket interface, and one subject was considered acceptable for demonstration purposes. Furthermore, the results obtained allowed the authors to explore the best way to present the data prior to larger studies.

2 Methods

2.1 The Participant

One male, right-sided, knee-disarticulation amputee participated in this study (age 29 years, height 178cm and mass 81kg). The participant had a stable residual limb volume, free from infection and inflammation, and was capable of conducting repeated, unassisted walking trials. The participant was fitted with a Pelite liner, a supra-condylar suspension socket, a KX06 polycentric knee and an Elan™ foot (Chas A Blatchford & Sons Ltd., Basingstoke, UK). A senior prosthetist verified the alignment of the prosthetic components and the fit of the socket prior to testing. This study was approved by the institutional Ethics and Research Governance Committee (ID: 12058 and ID: 6008).

2.2 Instrumentation

A gait laboratory was used to acquire the kinematic 3D motion at the residuum/socket interface, as detailed in previous work [16]. It was equipped with a two camera CODA motion analysis system (Charnwood Dynamics Ltd., Leicestershire, UK), an 8m level walkway and a 5° inclined walkway, also 8m in length. For both level and inclined walkways, a force plate (Model 9826BA, Kistler Instrument Ltd., Switzerland) was integrated and located approximately at the halfway points of each walkway. The motion analysis system collected the 3D marker data at 200Hz and three ground reaction force (GRF) components from the force plate at 500Hz.

In order to collect pressure and shear stress at the residuum/socket interface, a previously reported sensor system was used. Figure 1a illustrates the sensor system which incorporates three sensor units (SU) and a sensor system controller (SSC). The pressure and shear signals from the SUs are transmitted to the SSC and subsequently sent to a personal computer (PC) wirelessly via Bluetooth™ at 100Hz. A PC software was developed to collect, visualise and store the corresponding signals. The positive directions of the pressure (+ve P), circumferential shear (+ve S_C) and longitudinal shear stresses (+ve S_L) are also illustrated in Figure 1a. Prior to the amputee test, each of the SUs was calibrated as detailed in the authors' previous publication [21].

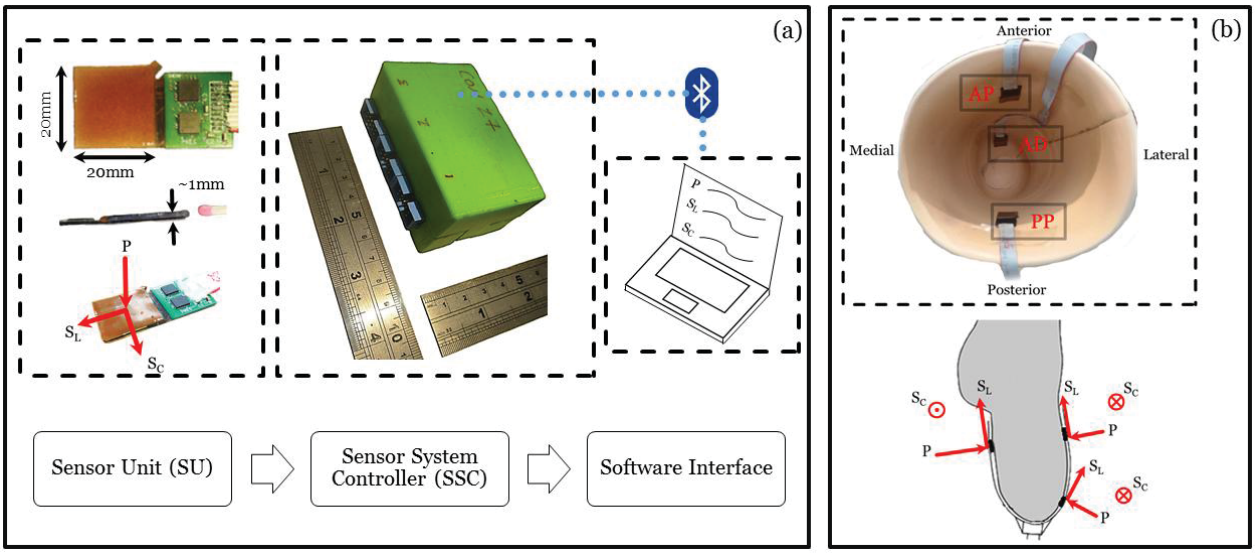

Figure 1: (a) Key components of the interface stress sensor system, incorporating three sensor units (SU) and a sensor system controller (SSC), which transmits SU outputs wirelessly to a laptop. The positive directions of the pressure (+ve P), circumferential shear stress (+ve S_C) and longitudinal shear stresses (+ve S_L) measured by an SU are shown by the red arrows. (b) Locations of the three SUs mounted on inner surface of the Pelite liner, corresponding to Anterior-Proximal (AP), Posterior-Proximal (PP) and Anterior-Distal (AD) locations of the residuum. Positive P and S acting at each location are indicated by red arrows.

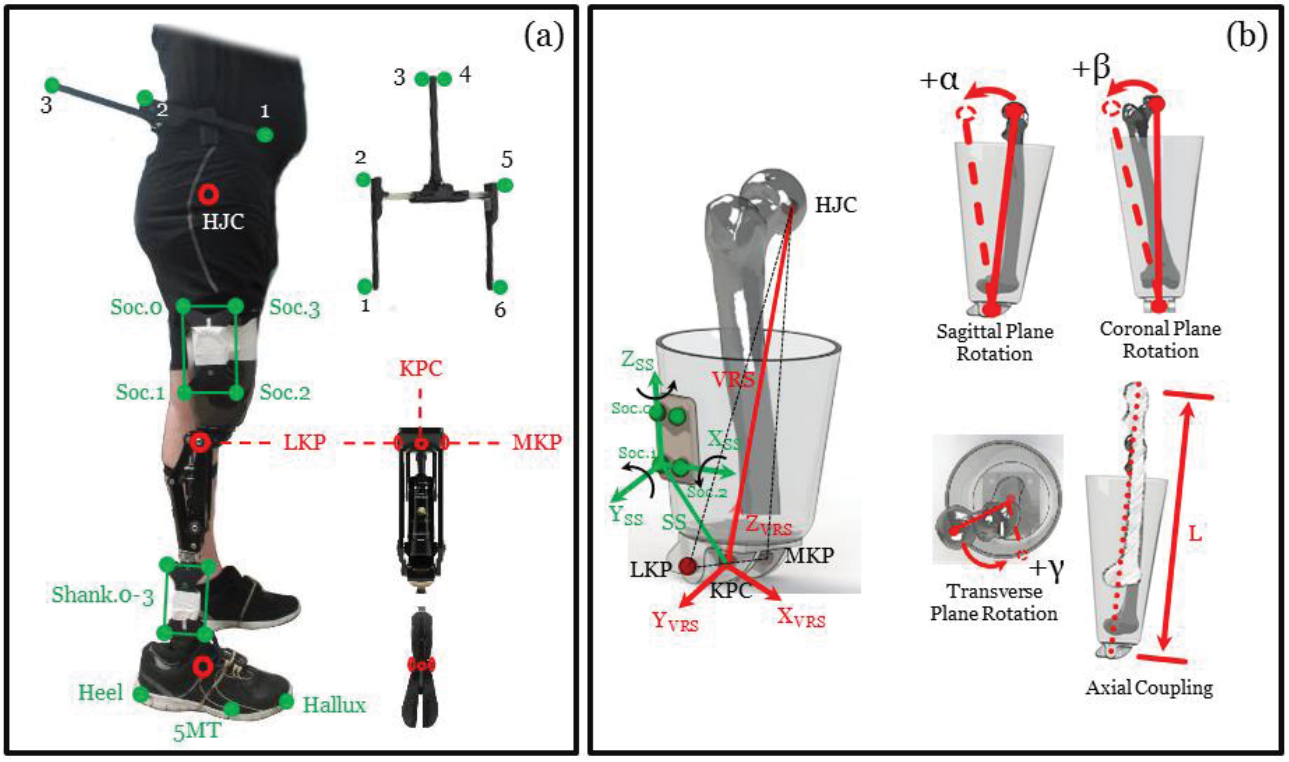

Figure 2: (a) Locations of real markers (shown by green dots) on the prosthetic side of the participant, including the pelvic frame used for tracking the pelvic motion. Locations of virtual markers (shown as red circles), including digitised markers and calculated markers. (b) An illustration of the residuum/socket interface coupling model and the corresponding angular and axial coupling derived from the model. The definitions of the VRS local co-ordinate system (X_{VRS}, Y_{VRS} and Z_{VRS}) and the SS local co-ordinate system (X_{SS}, Y_{SS} and Z_{SS}) are also indicated.

2.3 Protocols

Upon arrival, the participant was asked to doff the prosthetic socket and change into Lycra shorts. A total of 28 markers (Figure 2a) were then placed on both the prosthetic leg and the contralateral limb, by the investigator. Three SUs were then attached to the inner surface of the Pelite liner, by a senior prosthetist (Figure 1b). Subsequently, the amputee donned the socket and he was asked to walk on the level walkway, and then on the 5° descending and a 5° ascending walkway. Cadence was controlled by a metronome set at 100 beats per minute. For the tests carried out on each of the terrains, data were collected from 12 repeated trials with at least seven steps in each of the trials.

2.3.1 Marker Placement and Digitisation

The real marker placement and virtual marker tracking were based on the conventional six degree-of-freedom model. A frame consisting of six markers (marked as 1-6 in Figure 2a) was worn around the pelvis, tracking the pelvic movement. On the prosthetic side, a cluster of four markers (marked as Soc.0-Soc.3 in Figure 2a) was taped to the socket wall and was subsequently used to track the socket movement. Similarly, a cluster of four markers was mounted on the lateral-distal location of the prosthetic knee and was subsequently used to track the shank movement (marked as Shank 0-3 in Figure 2a). Three markers were attached to the shoe at locations equivalent to the heel, the fifth metatarsal and the hallux.

Virtual markers were digitised (Figure 2a) and estimated based on the location of the real marker placement. A pelvic model was defined using the digitised Anterior Superior Iliac Spine and Posterior Superior Iliac Spine landmarks and tracked in relation to the pelvic frame, during dynamic motion capture. The hip joint centres (HJC) were subsequently defined in relation to the pelvis [23, 24]. The lateral (LKP) and medial (MKP) ends of the prosthetic knee pivot were digitised on the prosthetic knee. The LKP and MKP virtual markers were tracked by using the socket cluster as the reference during dynamic motion capture. The location of the prosthetic knee pivot centre (KPC) was subsequently defined as the midpoint between these virtual markers.

2.3.2 Interfacial Sensor Placement

In order to measure the interfacial stresses at the residuum/socket interface, three SUs were placed at the anterior-proximal (AP), posterior-proximal (PP) and anterior-distal (AD) locations of the inner surface of the Pelite liner (Figure 1b), by a senior prosthetist. Based on the participant's feedback, these locations were considered to be the key load bearing areas. The three SUs were then connected to the SSC in order to produce simultaneous signals. Prior to the walking tests, all signals from each of the three SUs, with the socket doffed and in an unloaded state, were recorded to form baseline zero values.

2.4 Data Collection and Analysis

During each test, all real and virtual marker data, together with the three components of the GRF data, were recorded by the gait analysis system. The outputs of P, S_L and S_C from all SUs were also collected, simultaneously.

Data from clean trials were extracted for further analysis. These were defined as trials in which all key markers were visible to the CODA cameras and there was a complete single foot contact with the force plate. The data from the gait analysis system and sensors output were synchronised. This was implemented through a pulse issued by the motion capture system to the sensor system at the start of each trial, which triggered data acquisition of the sensor system instantaneously. The measured P, S_L, S_C from the SUs located at the AP, PP and AD locations were normalised by adopting the GCs and the detected gait events from the motion analysis system output.

2.4.1 GRF

Three components of GRF in the vertical (F_z), anterior-posterior (F_x) and medial-lateral (F_y) directions were recorded. In particular, +ve F_z represents the upwards direction, +ve F_x the anterior direction and +ve F_y the medial direction. The GRFs were used to determine the GC, as well as the gait events during stance phase i.e. initial contact (IC) and toe-off (TO). GRF values were compared for tests across different terrains and were also exploited to facilitate the discussion of the load transfer from the ground to the residuum/socket interface. Mean and one standard deviation (SD) values of GRF were calculated from the selected clean trials.

2.4.2 Residuum/Socket Interface Kinematics

The interface kinematics were analysed based on marker data, as detailed in previous work [16]. To review briefly, Figure 2b shows the definition of Virtual Residuum Segment (VRS) by linking the KPC and HJC, as well as the Socket Segment (SS) by linking KPC and one of the markers on the socket cluster. The local co-ordinate system was constructed to indicate the orientations of the VRS and SS, respectively. The VRS co-ordinate system has an origin at KPC and consists of X_{VRS}, Y_{VRS} and Z_{VRS} axes. Z_{VRS} represents the vector connecting KPC and HJC (Figure 2b). Y_{VRS} is perpendicular to Z_{VRS}, lying in the plane formed by HJC, LKP and MKP, pointing in the lateral direction. X_{VRS} is normal to the plane and points in the anterior direction. The SS co-ordinate system has an origin at Soc.1 and consists of X_{SS}, Y_{SS} and Z_{SS} axes. Z_{SS} represents the vector connecting Soc.1 to Soc.0, pointing in the proximal direction. X_{SS} represents the vector connecting Soc.1 to Soc.2, pointing in the anterior direction. Y_{SS} is normal to the plane formed by X_{SS} and Z_{SS} axes and points in the lateral direction. Subsequently, the dynamic angular couplings between VRS and SS in sagittal (α), coronal (β) and transverse planes (γ), during a GC, were characterised by calculating the Carden angle

between the VRS and SS, using their local co-ordinate systems [25]. According to the right hand rule, Figure 2b shows that +ve α, +ve β indicate the VRS rotation towards the posterior and medial regions of the socket, respectively, while +ve γ is defined as the VRS internal rotation relative to socket.

The dynamic axial coupling (L in Figure 2b) was assessed by calculating the real time length between KPC and HJC. The mean and one SD values for each of the angular and axial couplings, over a GC, were calculated from all clean trials.

2.4.3 Residuum/Socket Interface Kinetics

The mean and one SD values from all clean trials were calculated. In addition, the temporal P difference at the PP and AP locations, ΔP, was calculated according to Equation 1 and subsequently normalised by the values obtained at IC, with a positive value for ΔP indicating a higher P at the PP location. The P difference (ΔP) was then analysed with respect to angular coupling α, i.e. the VRS movement in sagittal plane, while S_L at the PP location were analysed with respect to the axial coupling L.

$$\Delta P = P_{PP} - P_{AP} \quad (1)$$

3 Results

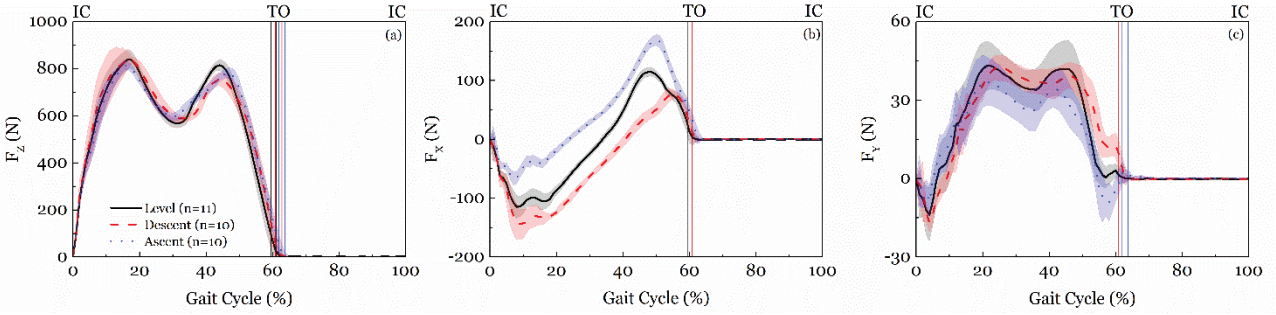

Figure 3: Mean and one standard deviation (SD) of ground reaction force (GRF) components, obtained during level, descent and ascent walking, over a gait cycle. (a) Vertical component (+ve F_z is defined as the upward direction), (b) anterior-posterior component (+ve F_x is defined as the anterior direction) and (c) medial-lateral component (+ve F_y is defined as the medial direction).

3.1 GRF

The three force components of the GRF, as a function of GC, when walking on different terrains are shown in Figure 3. F_z shows typical double-hump shaped profiles with mean peak forces of approximately 840N, 837N and 814N in early stance phase (10-20% of GC), and 814N, 754N and 781N in terminal stance (TS) (40-60% of GC) during level, descent and ascent walking, respectively (Figure 3a). Regardless of the terrain, the early stance phase peak and the TS peak in F_z were separated by a mid-stance local minimum, at approximately the same point in the GC (30%). This also corresponds to the maximum vertical position of the centre of mass during stance [26]. Therefore, this mid-stance point was chosen as a point of comparison for analysis in this work. F_x shows mean peak forces of approximately -115N, -145N and -66N in early stance phase, and +115N, +77N and +169N in the TS during level, descent and ascent walking, respectively (Figure 3b). F_y shows that mean peak forces of +42N, +40N and +37N during level, descent and ascent walking, respectively (Figure 3c).

3.2 Residuum/Socket Interface Kinematics

3.2.1 Angular Couplings

Figure 4 illustrates angular coupling in all planes i.e. α, β, γ as a function of GC. As a general trend exhibited on all terrains, α values of approximately -2° was indicated at IC (Figure 4a). It increase to peak values of approximately +7°, followed by a decrease in swing phase until finally restoring back to -2° for the next IC. At mid-stance (about 30% of GC), α reached approximately +1°, +2° and -2° during level, descent and ascent walking, respectively (Figure 4a). This was equivalent to a change in α of 3°, 4° and 0° compared to IC, during level, descent and ascent walking, respectively. In addition, a peak α of +7° was observed on all terrains, occurring during TS. This was equivalent to a change in α of 6°, 5° and 9° from the mid-stance point during level, descent and ascent walking, respectively.

Figure 4b shows angular coupling in the coronal plane (β). At IC, β values were generally at approximately -9° and gradually reached a negative peak value of approximately -12° at TS. β values were subsequently restored over the swing phase reaching approximately -8° at the next IC. Up to 4°, 4° and 3° change in β was observed in stance phase when walking on level, descending and ascending surfaces, respectively. In the transverse plane (Figure 4c), γ showed up to 1° variation over a gait cycle.

3.2.2 Axial Coupling

Figure 4d illustrates the dynamic axial coupling L over a GC. At IC, L values of approximately 482mm, 481mm and 476mm were evident during level, descent and ascent walking, respectively. From IC to TS, corresponding values of L deceased to values of approximately 455mm, 449mm and 461mm. Subsequently, L values increase over the swing phase to be restored to their original values at 100% GC.

3.3 Residuum/Socket Interface Kinetics

Figure 5a-c indicates the P, S_C and S_L values at the AP location. P values reveal a double-hump profile with the early stance peak values of approximately 32kPa, 32kPa and 33kPa, and TS peak values of 30kPa, 29kPa and 36kPa for level, descent and ascent walking, respectively. By contrast, the corresponding values for S_C (Figure 5b) and S_L (Figure 5c) were minimal with magnitudes of less than 2kPa across all terrains.

At the PP location, Figure 5d shows a typical double-hump shape for P in stance phase. In particular, a peak P of approximately 56kPa was obtained in early stance phase for all tests, while at TS, peak P of 53kPa, 50kPa and 58kPa were obtained for level, descent and ascent walking, respectively. S_L also revealed a double-hump profile during stance phase, with peak positive values in the early stance of 36kPa, 33kPa and 37kPa and at TS of 30kPa, 26kPa and 33kPa for level, descent and ascent walking, respectively. It is also noteworthy that the stresses at the PP location are in general higher than those measured at the AP location.

At the AD location (Figure 5g-i), there was a dramatic change in P and S profiles, particularly at TS. Peak P values of approximately 70kPa, 55kPa and 50kPa were evident (Figure 5g) during TS for level, descent and ascent walking, respectively. The peak values for S_C were approximately -26kPa, -15kPa and -24kPa (Figure 5h), while lower S_L (Figure 5i) peak values of -5kPa were recorded.

3.4 Correlation between the Interface Kinematics and Kinetics

The correlation between angular coupling in sagittal plane and interface stresses was evaluated by calculating the P differences (ΔP) from P values measured at the PP (Figure 5d) and AP (Figure 5a) locations. The corresponding ΔP and α values, as a function of the GC, are shown in Figure 6a. Positive values of ΔP were obtained during stance for all tests, indicating P at the PP location is always higher than P at the AP location

during the stance phase. The only -ΔP is evident during late stance during ramp ascent. Up to 11kPa, 12kPa and 7kPa values for ΔP were obtained during level, descent and ascent walking, respectively. The corresponding angular coupling in the sagittal plane, α, showed an increase of approximately -9° residuum rotation toward the posterior region of the socket during the stance phase, which was subsequently restored to 0° during the swing phase.

The correlation between axial coupling and interface stress measurement was evaluated by combining the longitudinal shear stresses, S_L (Figure 5f) and the corresponding axial coupling, L (Figure 4d) obtained at the PP location (Figure 6b). During most of the stance phase, positive S_L values were recorded, indicating movement of the residuum towards the distal aspects of the socket, which coincides with the decrease of L from 482mm at IC to 455mm during TS in the case of level walking. The decrease of L over a GC was particularly evident during both level walking and ramp descending.

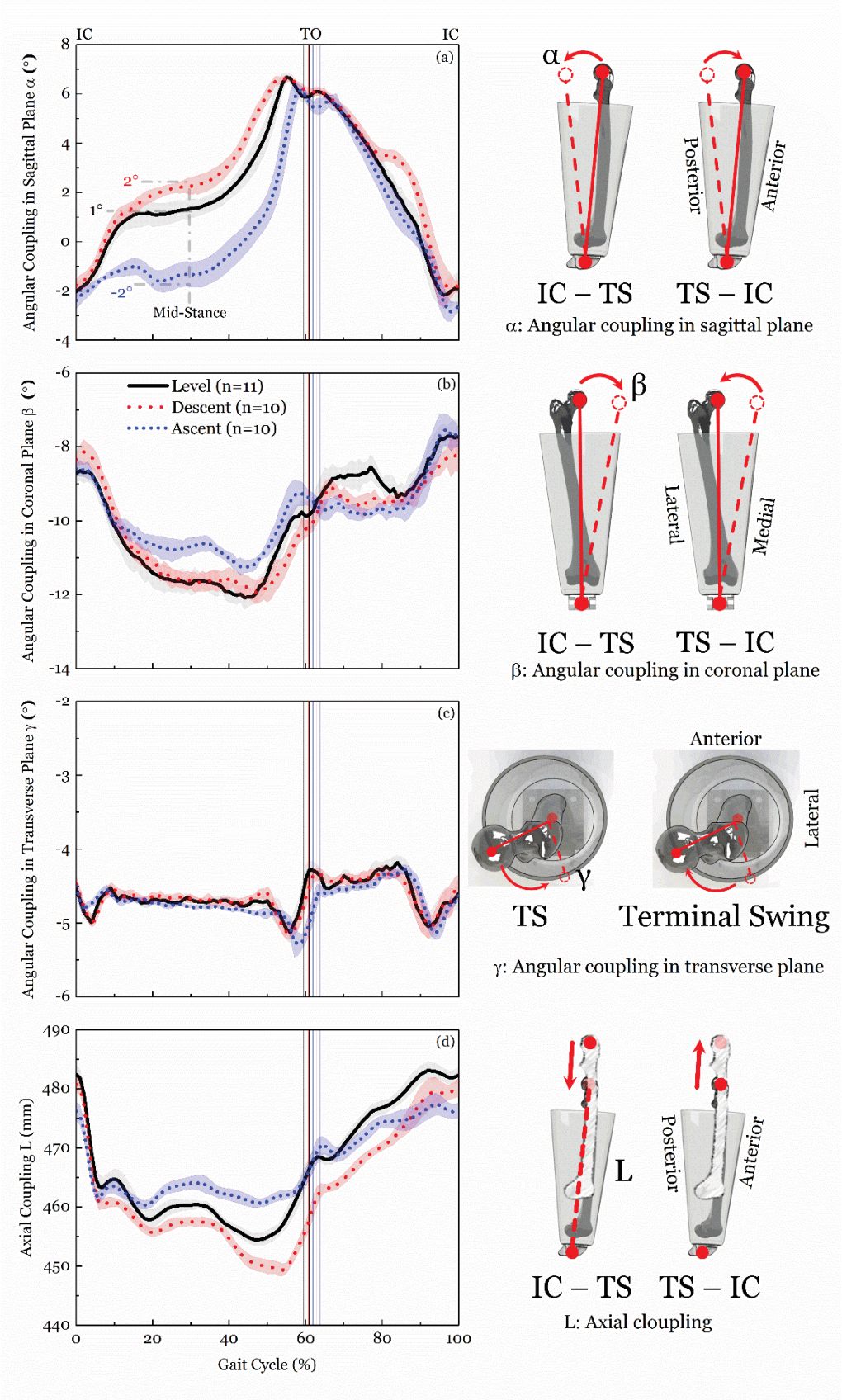

Figure 4: Mean and one standard deviation (SD) of angular coupling in the (a) sagittal plane, α, (b) the coronal plane, β, (c) the transverse plane, γ, and (d) and axial coupling L as function of GC, during level, descent and ascent walking. +ve α, +ve β and +ve γ are defined as VRS posterior, lateral, and internal rotation, respectively.

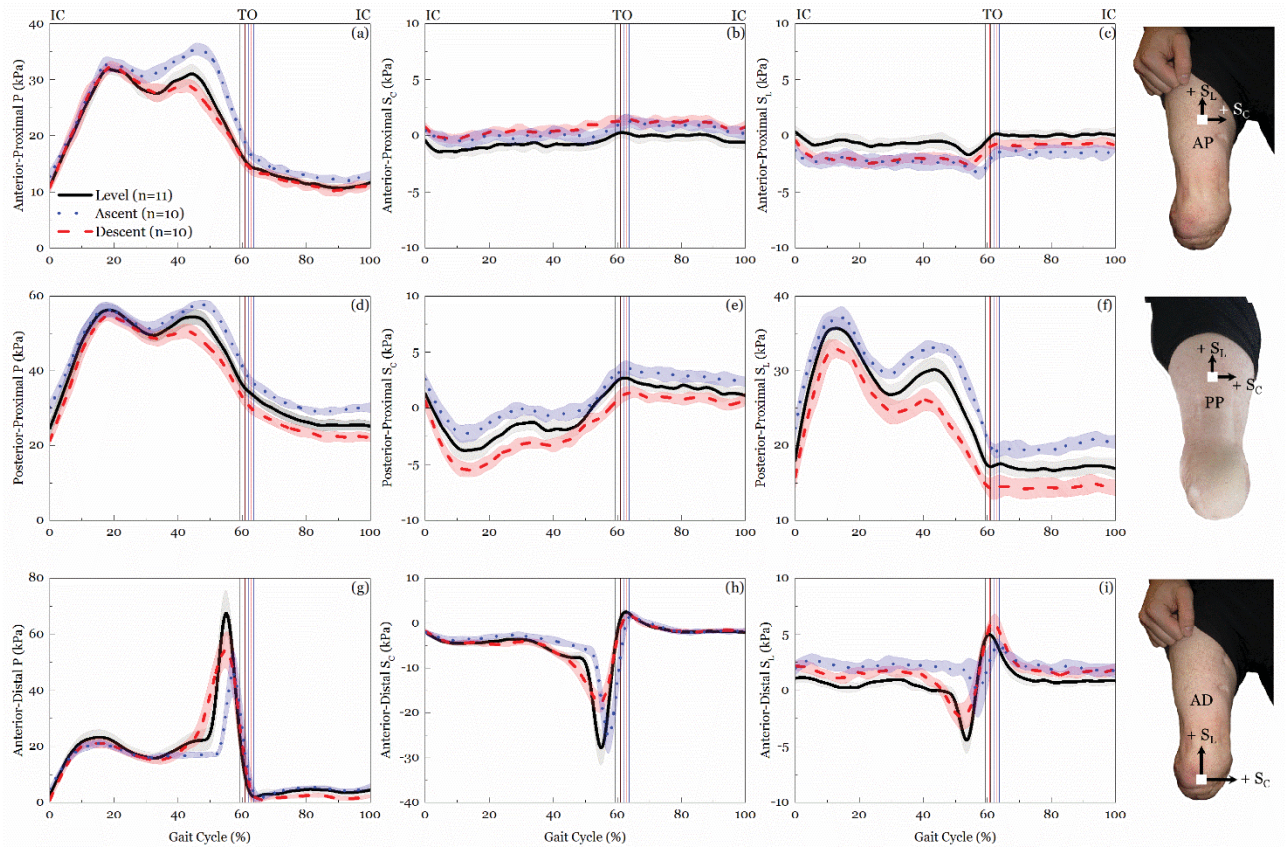

Figure 5: Mean and one standard deviation (SD) of pressure P, transverse shear S_C, longitudinal shear S_L measured from (a)-(c) the anterior-proximal (AP) location; (d)-(f) the posterior-proximal (PP) location; and (g)-(i) the anterior-distal (AD) location of the interface as function of gait cycle, during level, descent and ascent walking. +ve P is in the normal direction to the surface of the residuum. +ve S_C is circumferential shear in the medial direction (for the anterior sensors) and to the lateral direction (for the posterior sensor). +ve S_L is in the proximal direction. All definitions of +ve directions are also illustrated in Figure 1b.

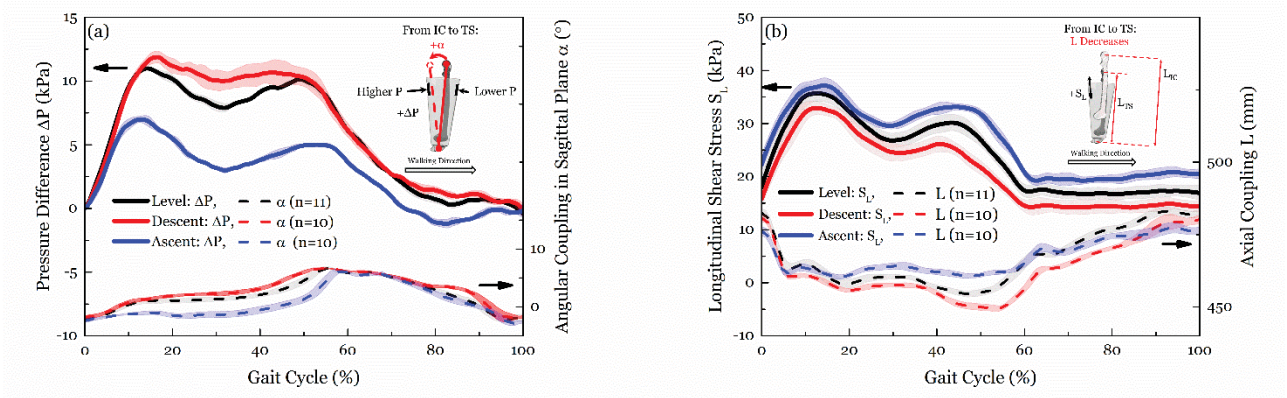

Figure 6: (a) Pressure difference (ΔP, on the left axis) between the PP location and the AP location, and the corresponding angular coupling (α, on the right axis) as a function of a gait cycle. (b) Longitudinal shear stress (S_L, on the left axis) at the PP location and corresponding axial coupling (L, on the right axis) over a gait cycle.

4 Discussion

This pilot study represents the first of its kind to present a combined assessment of kinematic and kinetic measurements at the lower limb residuum/prosthetic socket interface. By utilising 3D motion capture, the 3D relative motion between the residuum and the socket can be evaluated based on a new interface coupling model. At the same time, the corresponding interface kinetics including dynamic pressure and shear stresses were measured by using a novel interface stress sensor system. In this pilot study, both techniques were applied on a single knee-disarticulation amputee, thus minimising the factors associated with variations in socket fitting on different days, alignment perturbation, prosthetic componentry and the functionality of each individual amputee. The interface kinematics and kinetics and their dynamic correlation during the GC were studied based on data collected during amputee walking tests over level, descending and ascending surfaces, respectively.

4.1 GRF

Typical GRF profiles in all directions were obtained over the GC in Figure 3. In particular, F_Z (Figure 3a) presents double hump-profiles with the mean peak value of 840N in early stance phase and 814N during TS when walking on level surface, equivalent to the 81kg body weight of the amputee. Furthermore, the GRF from ramp descent (Figure 3b) shows the greater anterior-posterior braking force F_x (-145N) in early stance phase (10-20% of GC) when compared to that for level walking (-115N). This may be associated with the need of a greater braking force to oppose the component of the body weight acting down the slope. By contrast, GRF results obtained from ramp ascending (Figure 3b) reveals greater propulsive force (+169N) in the anterior-posterior direction at TS when compared to that from level waking (+77N). This may be associated with the demands of a greater propulsive force to oppose the component of the body weight acting down the slope. The positive F_Y (+37 - +42N) suggests that a medial force was acting on the foot during the stance phase (Figure 3c).

4.2 Correlation between the Angular Coupling and the Interface Stresses

In the sagittal plane, the kinematic movements and kinetic stresses at the interface were evaluated by characterising both the angular coupling in the sagittal plane i.e. α (Figure 4a) and the P at the AP and PP locations, on level, descending and ascending surfaces. For the kinematic coupling, α showed a 1° higher movement from IC to mid-stance when walking on descending surface (2°), compared with that on level walking (1°). This is likely due to the effort required in early stance phase to control the residuum, achieving foot-flat when descending the ramp. In addition, α showed 4° more movement from mid-stance to TS when walking on ascending surface (9°) when compared to that during level walking (5°). This may be affected by

the work produced by the hip in in TS to propel the limb forward to initiate the swing phase. The coupling seen is mainly a result of the moment applied to the socket as a result of the anterior-posterior component of GRF. For interface kinetics, during ramp descent, higher P at the PP and AP locations were obtained in early stance phase, comparing to that at TS. By contrast, when walking on the ascending ramp, higher P at the PP and AP locations were obtained at TS.

For the tests conducted on all terrains, +ve values for both α and ΔP were obtained during the majority of the stance phase (Figure 6a). In particular, the increase of α corresponds to the increase of ΔP in the early stance. This suggests that, in general, the larger the angular coupling i.e. α values, the higher P at the posterior region than at the anterior region. Such an effect is illustrated by the corresponding schematic in Figure 6a, showing the VRS engagement with the posterior region of the socket, while a higher P was obtained at the PP location compared to that at the AP location. It is well established that the PP location of the socket provides a seating interface for the knee-disarticulation amputee, especially during stance phase of the GC, to stabilise the trunk and the prosthetic knee [3, 22]. This effect was generally observed for all terrains. However, a greater α was observed during early stance phase when descending the ramp compared with the other two surfaces. This in principle corresponds to the greater anterior-posterior braking force (Figure 3b) during ramp decent in early stance phase, which may have resulted in a greater residuum rotation towards the posterior region of the socket from IC to mid-stance (Figure 4a). Indeed, at the two proximal locations, higher peak P were measured in early stance phase when compared to those at TS (Figure 5a and Figure 5d). By contrast, when ascending the ramp, a greater propulsion force was recorded during TS (Figure 3b). This may explain why the marked increase of α occurred in between mid-stance to TS of the GC. As a result, at the two proximal locations, higher peak P were measured at TS (Figure 5a and Figure 5d).

In the coronal plane, as indicated by the F_Y (Figure 3c), during most of the stance phase, a medially directed force was transmitted and exerted on the prosthesis. This provided a clockwise rotation of the residuum as it engaged with the medial region of the socket brim as illustrated in Figure 4b. The highest values of the angular coupling in the coronal plane, i.e. β were obtained during level walking, thus correlating with the peak magnitude of F_Y.

Significant changes in stresses were observed at the AD location of the residuum during the TS (Figure 5g - Figure 5i). This can be explained by the fact that the AD location acted like a kick point, as the amputee tried to propel the prosthesis forward in preparation for the swing phase. As a result, rotation between the residuum and socket could occur during this process. Indeed, an S_C of up to -26kPa was measured acting

354 laterally on the residuum. In a corresponding manner, up to 6° of residuum internal rotation in relation to SS
355 was determined during TS (Figure 4c).

356 4.3 Correlation between Axial Coupling and Interface Stresses

357 It is hypothesised that the change in the axial coupling length, a process often termed 'pistoning', could be
358 associated with the compressive and tensile loads applied to the residuum, as well as the vertical GRF in
359 stance phase, which is reflected by its typical double-hump shaped profile (Figure 3a). Longitudinal shear S_L
360 is directly linked to this 'pistoning' effect and, thus, a similar double-hump profile was also observed at the
361 PP location of the residuum (Figure 5f).

362 Figure 6b shows that, from approximately 0-20% of the GC, L shortened and the S_L at the PP location
363 increased. As gait progresses to mid-stance, both the L and the S_L stabilise to form a plateau-like region. L
364 further shortens after mid-stance phase with a subsequent increase in the S_L at the PP location. At TS, both
365 the L and the S_L started to recover. Limited S_L at the PP location was recorded during swing phase, although
366 the recovery of L was evident. This may be a direct result of bony movement inside the residuum, with
367 minimal resulting shear transmitted between the socket and the residuum. When walking on different
368 terrains, highest peak values of S_L were obtained during the ramp ascent, followed by the values measured
369 during level walking and ramp descent. However, the largest axial coupling was evident during ramp descent.
370 This is likely a result of load dependent non-linear friction behaviour, namely, the presence of slippage at the
371 residuum/socket interface.

372 4.4 Clinical Relevance

373 In this study, techniques for assessing socket interface biomechanics were demonstrated in relation to
374 walking on both level and ramped surfaces. The combined assessment of the kinematics and kinetics at
375 residuum/socket interface can potentially be used to evaluate the effects of a range of clinical interventions
376 on the residuum/socket interface biomechanics, such as the setting up of hydraulic ankle resistance and
377 different socket technologies. This approach could potentially be adopted in the design of adaptive sockets,
378 based on the socket movement in relation to the residuum and the corresponding interface stresses. Also,
379 prothetists could adopt the approach to assist socket fitting based on the kinematic and kinetic
380 measurements.

381

5 Conclusion

This paper presents a combined biomechanical assessment at residuum/socket interface using the kinematic and kinetic measurements based on two separate bioengineering techniques. Preliminary results suggest an association between the residuum movement, characterised by angular and axial coupling, and the pressure and shear stresses exerted at the residuum/socket interface. It is envisaged that such techniques could be potentially used to understand the biomechanical loading mechanisms at the residuum/socket interface, as well as to assist in the design and evaluation of a patient-specific prosthesis.

Conflict of interest

Dr. David Moser and Prof. Saeed Zahedi are employees of Chas A Blatchford & Sons Ltd. the manufacturer of the limb components used in this study.

Acknowledgments

The authors would like to thank the China Scholarship Council, the UK Engineering and Physical Sciences Research Council and Medical Research Council for support. All data supporting this study are openly available from the University of Southampton repository at http://doi.org/10.5258/SOTON/D0219.

Reference

[1] Mak AF, Zhang M, Boone DA. State-of-the-art research in lower-limb prosthetic biomechanics-socket interface: a review. J Rehabil Res Dev. 2001;38:161-74.

[2] Hagberg K, Branemark R. Consequences of non-vascular trans-femoral amputation: a survey of quality of life, prosthetic use and problems. Prosthetics and orthotics international. 2001;25:186-94.

[3] Radcliffe CW. Functional considerations in the fitting of above-knee prostheses. Artif Limbs. 1955;2:35-60.

[4] Narita H, Yokogushi K, Shii S, Kakizawa M, Nosaka T. Suspension effect and dynamic evaluation of the total surface bearing (TSB) trans-tibial prosthesis: a comparison with the patellar tendon bearing (PTB) trans-tibial prosthesis. Prosthet Orthot Int. 1997;21:175-8.

[5] Erikson U, James U. Roentgenological study of certain stump-socket relationships in above-knee amputees with special regard to tissue proportions, socket fit and attachment stability. Upsala J Med Sci. 1973;78:203-14.

[6] Lilja M, Johansson T, Oberg T. Movement of the tibial end in a PTB prosthesis socket: a sagittal X-ray study of the PTB prosthesis. Prosthet Orthot Int. 1993;17:21-6.

[7] Papaioannou G, Mitrogiannis C, Nianios G, Fiedler G. Assessment of amputee socket-stump-residual bone kinematics during strenuous activities using Dynamic Roentgen Stereogrammetric Analysis. Journal of biomechanics. 2010;43:871-8.

[8] Convery P, Murray KD. Ultrasound study of the motion of the residual femur within a trans-femoral socket during gait. Prosthetics and orthotics international. 2000;24:226-32.

[9] Sanders JE, Karchin A, Fergason JR, Sorenson EA. A noncontact sensor for measurement of distal residual-limb position during walking. J Rehabil Res Dev. 2006;43:509-16.

[10] Eshraghi A, Osman NA, Gholizadeh H, Karimi M, Ali S. Pistoning assessment in lower limb prosthetic sockets. Prosthet Orthot Int. 2012;36:15-24.

[11] Appoldt F, Bennett L, Contini R. Socket pressure as a function of pressure transducer protrusion. Bull Prosthet Res. 1969;10-11:236-49.

[12] Appoldt F, Bennett L, Contini R. Stump-socket pressure in lower extremity prostheses. Journal of biomechanics. 1968;1:247-57.

[13] Patterson RP, Fisher SV. The accuracy of electrical transducers for the measurement of pressure applied to the skin. IEEE transactions on bio-medical engineering. 1979;26:450-6.

[14] Williams RB, Porter D, Roberts VC, Regan JF. Triaxial Force Transducer for Investigating Stresses at the Stump Socket Interface. Medical & biological engineering & computing. 1992;30:89-96.

[15] Pearson JR, Holmgren G, March L, Oberg K. Pressures in critical regions of the below-knee patellar-tendon-bearing prosthesis. Bull Prosthet Res. 1973;10:52-76.

[16] Tang J, McGrath M, Laszczak P, Jiang L, Bader DL, Moser D, et al. Characterisation of dynamic couplings at lower limb residuum/socket interface using 3D motion capture. Med Eng Phys. 2015;37:1162-8.

[17] Papaioannou G, Mitrogiannis C, Nianios G, Fiedler G. Assessing residual bone-stump-skin-socket interface kinematics of above knee amputees with high accuracy biplane dynamic roentgen stereogrammetric analysis. 55th annual Meeting of Orthopaedic Research Society. Las Vegas, USA: Orthopaedic Research Society; 2009.

[18] Burgess EM, Moore AJ. A study of interface pressures in the below-knee prosthesis (physiological suspension: an interim report). Bull Prosthet Res. 1977;14:58-70.

[19] Appoldt A, Bennett L. A preliminary report on dynamic socket pressures. Bull Prosthet Res. 1967;10:20-55.

[20] Laszczak P, Jiang L, Bader DL, Moser D, Zahedi S. Development and validation of a 3D-printed interfacial stress sensor for prosthetic applications. Med Eng Phys. 2015;37:132-7.

[21] Laszczak P, McGrath M, Tang J, Gao J, Jiang L, Bader DL, et al. A pressure and shear sensor system for stress measurement at lower limb residuum/socket interface. Med Eng Phys. 2016;38:695-700.

[22] Radcliffe CW. Biomechanics of above knee prostheses. In: Murdoch G, editor. Prosthetic and Orthotic Practice. London: Edward Arnold; 1970. p. 191-8.

[23] Bell AL, Pedersen DR, Brand RA. A Comparison of the Accuracy of Several Hip Center Location Prediction Methods. Journal of biomechanics. 1990;23:617-21.

[24] Leardini A, Cappozzo A, Catani F, Toksvig-Larsen S, Petitto A, Sforza V, et al. Validation of a functional method for the estimation of hip joint centre location. Journal of biomechanics. 1999;32:99-103.

[25] Robertson G, Caldwell D, Hamill J, Kamen G, Saunders W. Three-Dimensional Kinematics. Research Methods in Biomechanics , 2E. Champaign, IL: Human Kinetics; 2014. p. 35-59.

[26] Burnfield J. Chapter3 Basic Functions. In: Perry J, Burnfield J, editors. Gait Analysis: Normal and Pathological Function. 2nd ed. New Jersey, US: Slack Incorporated; 2010. p. 42.